J Appl Electrochem (2011) 41:435–444
DOI 10.1007/s10800-010-0253-0

ORIGINAL PAPER

Effect of pre-treatment approach of a carbon support on activity of PtSn/C electrocatalysts for direct ethanol fuel cells

Jarupuk Thepkaew · Supaporn Therdthianwong · Apichai Therdthianwong

Received: 6 March 2010 / Accepted: 12 December 2010 / Published online: 25 December 2010

Abstract Vulcan XC-72R carbon was pretreated using acid and thermal activation methods, and the carbons obtained were used as supports for a PtSn/C catalyst synthesized by a successive reduction process. Surface characteristics of the supports, including BET surface area, pH_{PZC} and functional group, were analyzed using physical N_2 adsorption, mass titration, acid–base titration, and Fourier transform infrared (FTIR) spectrometer technique, respectively. The prepared PtSn/C catalysts were characterized by X-ray diffractometer (XRD), energy dispersive X-ray spectrometer (EDX), inductively coupled plasma–atomic emission spectrometry (ICP–AES), and transmission electron microscope (TEM) techniques, and then were examined for their behavior under ethanol oxidation as well as for their performance in a direct ethanol fuel cell (DEFC). The results showed that pretreatment by HNO_3 produced various oxygenated functional groups on the support surface and increased its acidic property. The strong acidity of the acid-treated support led to an unfavorable condition for the Pt reduction reaction and resulted in low Pt content but high Pt:Sn ratio in the PtSn/C catalyst. On the other hand, thermal activation increased the base functional groups on the carbon surface, which enhanced reduction of Pt precursor, and consequently, provided a small average metal particle size of 2.2 nm. The results from cyclic voltammetry, chronoamperometry and cell performance testing confirmed that the catalytic activity for ethanol oxidation and the performance in the direct ethanol fuel cell of the heat-treated carbon-supported PtSn catalyst was superior to the fresh PtSn/C catalyst and the acid-treated carbon-supported PtSn catalyst.

Keywords Direct ethanol fuel cells · PtSn/C · Ethanol oxidation · Pre-treatment · Carbon support

J. Thepkaew · S. Therdthianwong (✉)
Department of Chemical Engineering, Faculty of Engineering, King Mongkut's University of Technology Thonburi, 126 Pracha-Uthit Road, Bangmod, Tungkru, Bangkok 10140, Thailand
e-mail: supaporn.the@kmutt.ac.th

A. Therdthianwong
Fuel Cells and Hydrogen Research and Engineering Center, Clean Energy System Group Pilot Plant Development and Training Institute, King Mongkut's University of Technology Thonburi, 126 Pracha-Uthit Road, Bangmod, Tungkru, Bangkok 10140, Thailand

1 Introduction

In the last decade, direct alcohol fuel cells (DAFCs) have become particularly attractive power sources for mobile applications. This kind of fuel cell uses alcohol solutions, containing methanol or ethanol, which is fed directly into the cell. In contrast to hydrogen feed fuel cells, such as the proton exchange membrane fuel cell (PEMFC), DAFCs exhibit no problems with handling, fuel storage, transportation or distribution [1, 2]. Since no reformer is required, this fuel cell system is also simpler and cheaper. Methanol is considered to be one of the most promising fuels for DAFCs, as it can be effectively oxidized to produce CO_2 and water as the waste products. However, concerns about fuel crossover problems as well as methanol's toxicity to the optical nerves of humans have made ethanol a strong candidate for an alternative liquid fuel [3]. As well as being safer, ethanol has numerous benefits, such as high energy density (8.01 kWh kg^{-1} in contrast to 6.09 kWh kg^{-1} of methanol), renewability and natural availability from the fermentation of biomass resources, which does not release greenhouse gases into the atmosphere [1]. Due to the C–C

bonds in an ethanol molecule, the pathway of the ethanol's oxidation reaction (EOR) is more complicated than that of methanol [1, 4]. Breaking C–C bonds is very difficult at low operating temperatures. Consequently, the final products of oxidation consist mainly of acetaldehyde and acetic acid, which lead to a decrease in the fuel cell's efficiency [4–7].

One way to enhance the EOR is modification of well-known Pt catalysts by introducing a second metal, such as Ru [8–10], Sn [4, 8, 11–13], W [8, 14], Mo [8, 15], and Rh [16, 17], as an alloying metal since the second metal can promote the dissociation of water to form the OH-species for oxidative CO removal at a lower potential than unalloyed Pt can ($0.6\ V < E < 0.8$ V/RHE) [9]. As reported in previous studies [8, 18–20], PtSn/C catalysts have higher activity towards EOR than the other binary catalysts. Recently, Jiang and co-workers [21] have discovered that the PtSn/C catalyst prepared by a successive reduction procedure could considerably increase catalytic activity for EOR and DEFC performance more than the conventionally modified polyol synthesis could. This is due to the catalyst having sufficient surface OH-species to oxidize the poisoning CO-adsorbed species and free Pt active sites for further ethanol adsorption.

The otherwise expensive Pt can be well dispersed on a high surface area substrate to attain high utilization of noble metals. Vulcan XC-72R carbon is widely used as a support for Pt catalysts in low-temperature fuel cells due to its low cost and high availability [22]. It also has both a high surface area and adequate electrical conductivity to act as a path for electron flow. The activities of catalysts could be strongly affected by the dispersion effect as well as the interaction effect between the metal precursors and the support materials [23]. Thus, the supports are generally activated before their use to increase metal dispersion and catalytic activity. The activation approaches have been classified as oxidative treatment and thermal treatment. Pre-treatment of carbon supports for low-temperature fuel cells was reviewed by Antolini [22], who disclosed that the chemical pre-treatment by acids, bases, or oxidizing agents could alter surface functional groups of carbon, depending upon the nature of the oxidants. For thermal pre-treatment of carbon under inert atmosphere at high temperature, the impurities present on the carbon surfaces could be efficiently removed, leading to an increase in the active surface area of the carbon. However, the effect of the oxidative/thermal activation methods of carbon supports on the EOR has not been fully studied.

In this research study, two pretreatment methods, acid and thermal treatments, were used to prepare Vulcan XC-72R carbon support. Then PtSn was synthesized by a successive reduction process [21]. The PtSn/C catalysts obtained were characterized for EOR using cyclic voltammetry and chronoamperometry techniques, and DEFC performance testing.

2 Experimental

2.1 Carbon support

2.1.1 Pretreatment

Vulcan XC-72R carbon black (Cabot Corp.) was first pre-treated by chemical/thermal treatment. For chemical treatment, 5 M HNO_3 was added to the fresh carbon, which was then heated at its boiling point for 5 h. Afterward, the solution was centrifuged, washed with copious amounts of deionized water, and dried at 150 °C overnight. For thermal activation, the virgin carbon was heated at 600 °C under N_2 atmosphere for 30 min [23]. The HNO_3-treated and heat-treated carbon supports were denoted as NA-C and HT-C, respectively.

2.1.2 Characterization

The fresh and treated supports were characterized using an Autosorb-1 (QuantaChrome Co. Ltd.) to determine their specific surface areas (S_{BET}) and textural properties. The physical adsorption was conducted at −196 °C using N_2 as an adsorbent. The pH at the point of zero charge (pH_{PZC}) of the supports was estimated by a mass titration method explained in detail by Reymond et al. [24]. Three different initial pH solutions of 0.1 M KNO_3 used were 4, 6, and 9. Varying amounts of the support, i.e. 0.05, 0.5, 5, 10, and 15% by weight, were subsequently added to those initial pH solutions. The equilibrium pH was measured after 24 h by a pH meter, model 59003-25 (Cole-Parmer Instrument Co.). The surface functional groups of the fresh and pre-treated Vulcan XC-72R were carried out by a Spectrum One FT-IR Spectrometer (Perkin Elmer Co.). The solid samples were first milled with potassium bromide (KBr), and then compressed into thin pellets. A frequency range between 500 and 4000 cm^{-1} with a resolution of 4 cm^{-1} was used. The acid and base sites on the support surfaces were determined by titrating with NaOH and HCl, respectively [25]. In details, 0.1 g of sample was added to 50 mL of either 0.1 M NaOH or 0.1 M HCl. The solution was then shaken at room temperature for 24 h. Thereafter, the suspension was filtered and titrated with either 0.1 M HCl or 0.1 M NaOH.

2.2 PtSn/C electroatalysts

2.2.1 Preparation

The PtSn/C electrocatalysts were prepared by a successive reduction procedure as described in the literature [21, 26]. In brief, SnO_2 colloid was initially prepared by dissolving stannous chloride dihydrate ($SnCl_2{\cdot}2H_2O$, Sigma-Aldrich, Inc., 98%) in analytical grade ethylene glycol (Sigma-

Aldrich, Inc., 98%). Then, the slurry was heated up to 190 °C and kept at this temperature until the solution became a colloid slightly yellow in color. The required amount of SnO_2 colloid was added to chloroplatinic acid hexahydrate ($H_2PtCl_6{\cdot}6H_2O$, Sigma-Aldrich, Inc., 37 wt% Pt content) with continuous stirring for 15 min. Afterwards, the pH of the solution was adjusted above 11 with 1 M NaOH. The mixture was heated to 160 °C and kept at this temperature for 2 h while passing N_2 through the system to eliminate oxygen and organic byproducts. The dispersed Vulcan XC-72R pre-treated with the different methods was then added to the solution; and was further stirred for 2 h. Finally, the solution was centrifuged, washed with copious amounts of DI water until no detection of chloride anion remained, and dried in an air oven at 120 °C overnight. The ratio of platinum and tin taken for the catalyst preparation was 3:1. The metal loading of all catalysts was 20 wt%. The as-prepared catalysts were designated as PtSn/C where C referred to F-C for fresh, NA-C for HNO_3-treated and HT-C for heat-treated Vulcan XC-72R.

2.2.2 Physical characterization

The characterization of the particle size and the crystalline structure of the as-prepared catalyst samples was carried out by an X-Ray Diffractometer (Bruker AXS Model D8 Discover) using a Cu Kα radiation source. The XRD patterns were recorded from 15° to 90° at the scan rate of 0.03° min^{-1}. Actual content of Pt and Sn in the catalysts was obtained using inductively coupled plasma–atomic emission spectrometry (ICP–AES) technique with an OPTIMA 3000 (Perkin Elmer Co.). Transmission electron microscope (TEM) technique was used to examine morphology and metal particle sizes. The sample was dispersed in ethanol and then deposited on the copper grid. TEM images were taken using a JEOL 2010 electron microscope operating at 100 kV. More than 300 particles were counted to obtain the average metal particle sizes and size distribution of all catalysts. The energy dispersive X-ray spectrometer (EDX) analysis was conducted using an X-ray detector in a scanning electron microscope (JSM-6400 attached with EDX Oxford Link ISIS series 300, JEOL) with the working voltage held at 20 kV.

2.2.3 Electrochemical test

Electrochemical measurements of the catalysts were carried out by cyclic voltammetry and chronoamperometry techniques using a potentiostatic/cyclic voltammetry (Solartron SI 1287). A working electrode was prepared by ultrasonically dispersing the synthesized catalysts in a solution of 5 wt% Nafion ionomer (Electrochem. Inc.) and analytical grade isopropanol for 1 h. A 25 μL of the suspension was then dropped, at 100 μg catalyst/cm^2 loading, on a clean glassy carbon electrode with a diameter of 3 mm (BAS Inc.). The same electrochemical measurement was also carried out for all the electrocatalysts but with the same Pt loading in all the electrodes. Pt gauze of 1 cm^2 was used as a counter electrode while a saturated calomel electrode (SCE) was used as a reference electrode. The electrolytes for hydrogen and ethanol oxidation were a 0.5 M H_2SO_4 and a 0.5 M H_2SO_4 containing 1 M CH_3CH_2OH solution, respectively. Before performing the measurement set at a constant temperature of 25 °C, the electrolytes were saturated with high purity Ar for 30 min to expel oxygen in the solutions. All cyclic voltammograms were recorded versus SCE. Electrochemical surface area (ESA) of the Pt-based catalysts evaluated from hydrogen adsorption or desorption area normally represents available Pt active sites, which could be calculated using the following equation [27]:

$$\mathrm{ESA} = 0.1 \times \frac{Q_{\mathrm{ads}}}{Q_{\mathrm{ref}} \times L_{\mathrm{Pt}}} \quad (1)$$

where Q_{ads} is the charge of hydrogen adsorption, commonly equivalent to hydrogen desorption (mC cm^{-2}), Q_{ref} refers to the hydrogen desorption charge of the Pt single crystallite (0.21 mC cm^{-2}), and L_{Pt} is the Pt loading (mg cm^{-2}).

2.3 MEA preparation and single cell test

The anode electrodes were prepared using the synthesized PtSn/C catalysts. First, the catalyst was suspended in a mixture of 5 wt% Nafion® solution (Electrochem Inc.) and isopropanol for 2 h. The Nafion content of 33 wt% was used for all catalysts. The slurry was then applied onto the commercial carbon cloth based ELAT® (E-TEK) by painting method. A commercial GDE with Pt/C catalyst (E-TEK) was used for the cathode side. The metal loading in all the electrodes for the anode sides was kept at 1.8 mg cm^{-2}. To remove organic impurities as well as to promote a protonic form, the Nafion® 115 membrane (DuPont) was treated in the following solutions: deionized water, 3 wt% H_2O_2, deionized water, 0.5 M H_2SO_4, and deionized water, respectively as described in the previous work [27]. The membrane electrode assembly (MEA) was fabricated by hot-pressing at 150 °C and 6.9×10^6 Pa for 150 s. A single cell was assembled with the prepared MEA and graphite bipolar plates and placed in a commercial PEMFC single cell housing (5 cm^2 purchased from ElectroChem Inc.). A solution of 1 M CH_3CH_2OH was fed to the anode at the flow rate of 1 mL min^{-1}. Unhumidified O_2 at the flow rate of 100 mL min^{-1} and 2×10^5 Pa was the oxidant supplied to the cell. The cell temperature was set at 90 °C.

3 Results and discussion

3.1 Physical characterization of pretreated supports

Specific surface area (S_{BET}) and pore volume of the supports before and after pre-treating with the different activation approaches are summarized in Table 1. It can be seen from Table 1 that these activation methods affected the specific surface areas and textural characteristics of the supports differently. The HNO_3 treatment did not alter the surface area of the supports, which is in accordance with what was reported in previous literature [28, 29]. This treatment also hardly modified the pore structure of the Vulcan XC-72R; however, it increased the meso-pore volume. In contrast, thermal treatment improved the BET surface area by approximately 37% and generated micropores, resulting in reduction of the average pore radius. This reduction could have been due to the removal of inorganic matter on the support surface at high temperature, a result that was also found by Coloma et al. [30].

Table 1 also shows the pH value at the point of zero charge (pH_{PZC}) of the supports. The pH_{PZC} indicates the surface oxygen complexes and surface charges of the support. The latter determines the strength of the interaction between the metal precursors and the support surface during the deposition procedure. The complex species on the support surface can generally be classified as acidic groups (carboxylic, anhydride, and lactone), neutral or weakly acidic groups (phenolic, carbonyl, quinone, and ether), and basic groups (pyrone and chromene) [28]. The surface of the fresh carbon (F-C) was considered to be amphoteric with pH_{PZC} of 7.05, meaning that it can adsorb either anionic or cationic species depending on the pH of the solution. The HNO_3 treatment introduced acidic property in NA-C whereas HT-C showed the basic property.

The acidity of NA-C may result from the acidic groups generated from an oxidized complex species of HNO_3. As a result, the pH_{PZC} of the nitric-treated carbon was lower. The basic characteristic of HT-C was attributed to the pyrolysis of acidic oxygen surface groups to form pyrone-type groups when exposed to air at room temperature [30]. In addition, the acid–base surface values shown in Table 1 confirmed that the base functional groups on F-C and HT-C are higher than that of NA-C. It can be clearly seen that the pretreatment method could alter functional groups as well as the microstructure of the carbon. Consequently, the Pt adsorption capacity of the heat-treated support was affected.

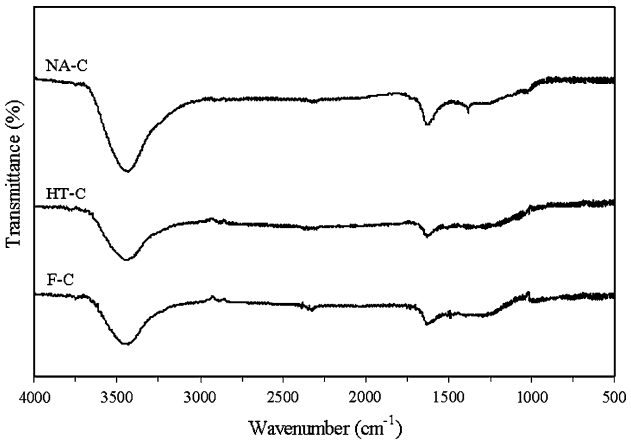

Fig. 1 FTIR spectra of the various supports

The surface functional groups of the Vulcan XC-72R before and after HNO_3/thermal treatment were characterized using FTIR technique. Their FTIR spectra are illustrated in Fig. 1. It can be seen that there were two obvious characteristic peaks at 3430 and 1630 cm^{-1} present on the surfaces of F-C. These two bands are assigned to phenol group and quinone group, respectively [12, 25, 31, 32]. Heating up to 600 °C under an inert atmosphere could remove some of less stable oxygen complexes, as shown by the slight decrease in the intensity of the characteristic FTIR bands of HT-C [32]. In contrast, the HNO_3 activation approach increased a large number of the phenol and quinone groups on the support surfaces. In addition, a sharp absorption peak at 1380 cm^{-1} associated with carboxyl-carbonates and nitrate groups was observed [29]. Thus, it can be deduced that several functional groups such as phenol, quinone, carboxyl-carbonates, and nitrate groups were produced on the carbon surface by HNO_3 treatment. These results are in agreement with the pH_{PZC} and the acid values of the supports.

3.2 Physical characterization of PtSn/C catalysts

The XRD patterns of all the as-prepared PtSn/C catalysts and the commercial Pt/C catalyst supplied by E-TEK are

Table 1 Some characteristics and adsorption parameters of supports

Support	S_{BET} (m^2 g^{-1})	Pore radius (Å)	V_{total} (mL g^{-1})	V_{micro} (mL g^{-1})	V_{meso} (mL g^{-1})	pH_{PZC}	Acid value (meq g^{-1})	Base value (meq g^{-1})
F-C	193	38.8	0.374	0.16	0.214	7.05	464	244
NA-C	202	39.9	0.403	0.16	0.243	2.47	683	160
HT-C	265	34.1	0.452	0.22	0.232	8.99	404	328

shown in Fig. 2. The broad diffraction peak at around 25°, assigned to the graphite (002) plane of the hexagonal structure of Vulcan XC-72R, were observed in all diffractograms. Four typical diffraction peaks of a crystalline Pt face-centered cubic (fcc) phase including Pt(111), Pt(200), Pt(220), and Pt(311) obviously appeared at about 39°, 46°, 67°, and 81°, respectively. Neither the diffraction peaks of tin metallic nor those of tin oxide were found in the prepared PtSn/C catalysts (See curves b, c, d). Previous literature reported that [7, 21] SnO_2 diffraction peaks at around 34° and 52° were present in PtSn/C catalysts prepared by successive reduction methods, but at low SnO_2 content, the peaks could not be observed [7]. However, in this study, the as-prepared PtSn/C catalysts, the non-alloyed PtSn was formed as indicated by the unchanged positions of the Pt diffraction peaks [See especially Pt(111)] from those of the Pt/C catalyst [21]. Considering the ratio of Pt:Sn of all catalysts and a commercial Pt_3Sn/C obtained from EDX and ICP analysis as shown in Table 2, it was in the range of 2.68–7.53 and 10.15–21.11, respectively. The Pt:Sn ratio of the commercial electrocatalyst obtained from EDX technique was pretty much closer to the prescribed value of 3:1. The Pt:Sn ratio of the prepared samples are higher than the intended values indicating that they contain small Sn content as also found in the XRD results.

The TEM images of all the synthesized PtSn/C catalysts, where the metal particles are identified by black spots, are shown in Fig. 3. The effects of the support pre-treatment methods on Pt particle sizes of the PtSn/C catalysts and their size distribution can be estimated. The PtSn/HT-C catalyst gave the smallest metal sizes as compared with the other prepared PtSn/C catalysts, owing to higher surface area of heat-treated support. However, some aggregation of the metal particles, possibly leading to bigger metal sizes

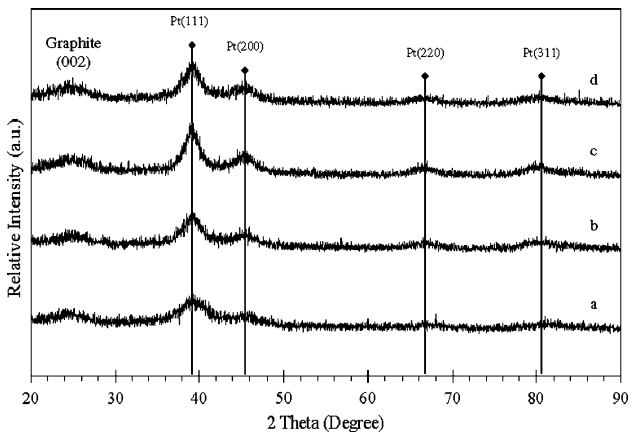

Fig. 2 X-ray diffractograms of the Pt-based catalysts: **a** Pt/C (ETEK), **b** PtSn/F-C, **c** PtSn/NA-C, **d** PtSn/HT-C

Table 2 TEM mean particle sizes, surface and gross Pt:Sn rations of various PtSn-based catalysts

Sample	Mean particle size (nm)	Pt:Sn	
		EDX	ICP–AES
Pt/C (ETEK)	2.1 ± 0.4 [27]	na	na
PtSn/F-C	2.6 ± 0.7	7.53 ± 3.7%	21.11
PtSn/NA-C	2.5 ± 0.6	4.74 ± 10.5%	10.15
PtSn/HT-C	2.2 ± 0.5	5.46 ± 3.1%	13.58
PtSn/C (commercial)	na	2.68	16.14

and wider size distribution (1.5–6.0 nm), was clearly observed in the PtSn/F-C catalyst. Pt size distribution of PtSn/NA-C and PtSn/HT-C catalysts was narrower with the particle size range of 1.5–4.5 nm. The mean particle sizes of Pt calculated from the TEM images of all catalysts are displayed in Table 2, demonstrating the mean particle sizes of all catalysts in the range of 2.1–2.6 nm. It was observed that all the binary catalysts had bigger metal particle sizes than that of Pt/C catalyst. The average diameters of PtSn/F-C, PtSn/NA-C and PtSn/HT-C catalysts were 2.6, 2.5, and 2.2 nm, respectively. Additionally, the pre-treatment approaches of the support affected metal dispersion in these as-prepared PtSn/C catalysts. In comparison to PtSn/F-C and PtSn/NA-C catalysts, Pt particles of the PtSn/HT-C catalysts are uniformly well-dispersed on the support as shown in Fig. 3c.

As already mentioned, functional groups on support surface could manipulate the Pt adsorption of the support surface, leading to different Pt contents in the prepared PtSn/C catalysts. The ICP analysis showed that the adsorbed Pt contents in PtSn/F-C, PtSn/NA-C and PtSn/HT-C catalysts were 13.1, 9.1, and 10.2 wt%, respectively. Higher amounts of Pt adsorbed on the basic HT-C and amphoteric F-C than that on the acid NA-C could be attributed to the surface charge of the support. The higher base values of both F-C and HT-C than that of NA-C shown in Table 1 indicated higher base functional groups on the surfaces of the supports. The Pt deposition to the support surface was enhanced by the base functional groups where Pt reduction can occur. It was reported in other work that base condition was preferable in the preparation of Pt nanoclusters-deposited supports because the reduction process of the Pt precursor was best affected under base condition [25]. Furthermore, the small Pt nanocluster size for PtSn/HT-C might have originated with well distributed base functional groups. The reason why F-C could adsorb Pt more than HT-C is that the surface oxygen groups presented on F-C can act as anchoring centers for the metal precursors and these complex surface oxygen species was subsequently decomposed to form pyrone-type groups after the heat treatment.

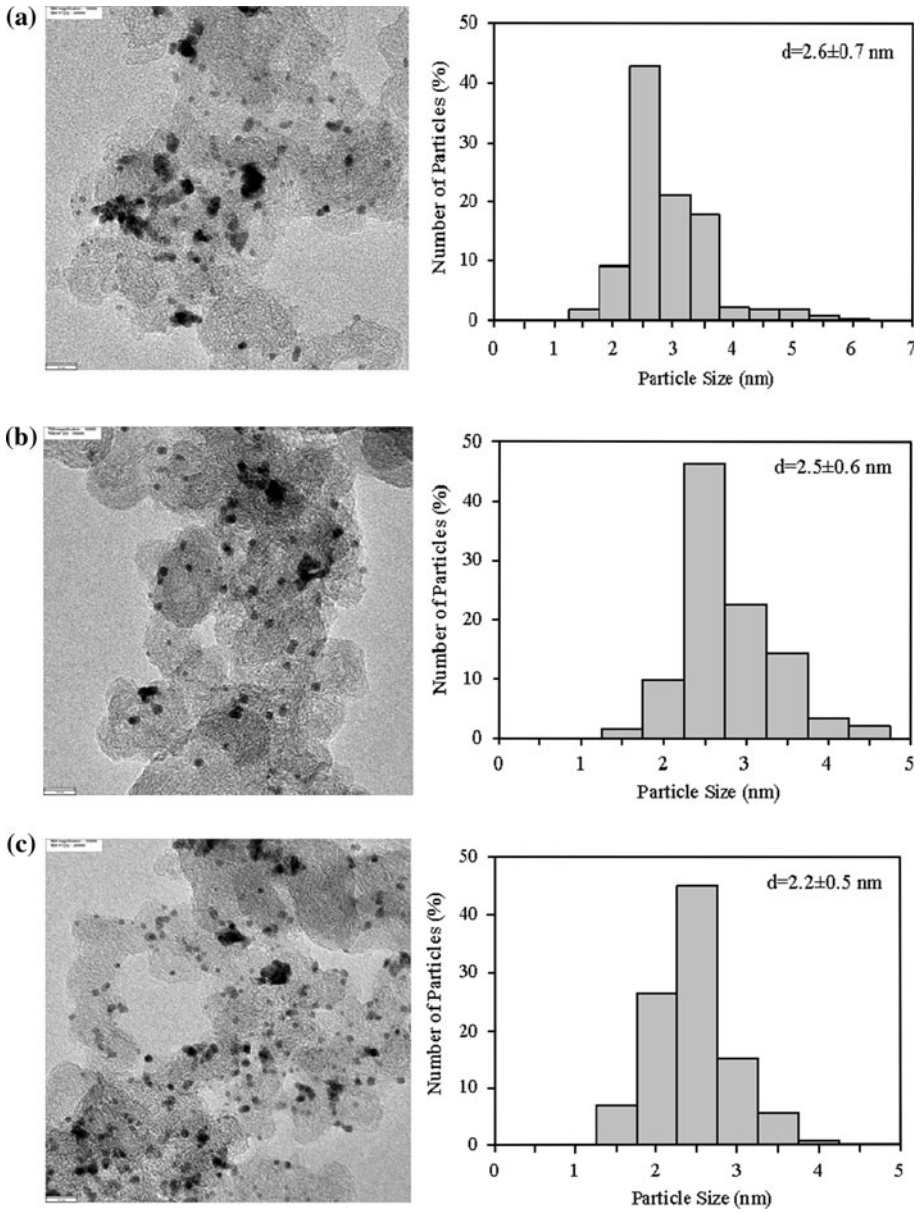

Fig. 3 TEM images and size distribution of the as-prepared PtSn/C catalysts: **a** PtSn/F-C, **b** PtSn/NA-C, **c** PtSn/HT-C

3.3 Electrochemical characterization and activity of PtSn/C towards EOR

Cyclic voltammograms of the as-prepared PtSn supported on the different pre-treated supports in 0.5 M H_2SO_4 electrolyte are illustrated in Fig. 4. The current responses in the potential range of −200 to 800 mV/SCE for all voltammograms were normalized by the actual Pt contents evaluated from ICP analysis as being in the unit of mA $mgPt^{-1}$. In the absence of ethanol solution, only the adsorption and desorption of hydrogen and oxygen were appeared. The hydrogen ad/desorption regions of all the Pt-based catalysts were seen in the potential range of −200 to 100 mV/SCE. A larger double-layer charging current of PtSn/NA-C than that of the untreated and heat-treated PtSn/C catalysts was observed. This is attributed to the presence of the surface oxygen complexes formed from the dissociation of water on the Sn sites as well as the oxidation of the support by the acid treatment, thereby increasing the electrode capacitance [33]. It was believed that the preferential oxygen-containing species facilitated the removal of the strongly CO-adsorbed species to free Pt active sites. As a result, PtSn/NA-C catalyst was expected to provide the highest catalytic activity for ethanol oxidation. On the other hand, in regard to the electrochemical surface area (ESA), the catalysts could be ranked in the following sequence: PtSn/HT-C (52.9 $m^2\ g^{-1}$) > PtSn/F-C (14.4 $m^2\ g^{-1}$) > PtSn/NA-C (9.3 $m^2\ g^{-1}$). PtSn/HT-C had

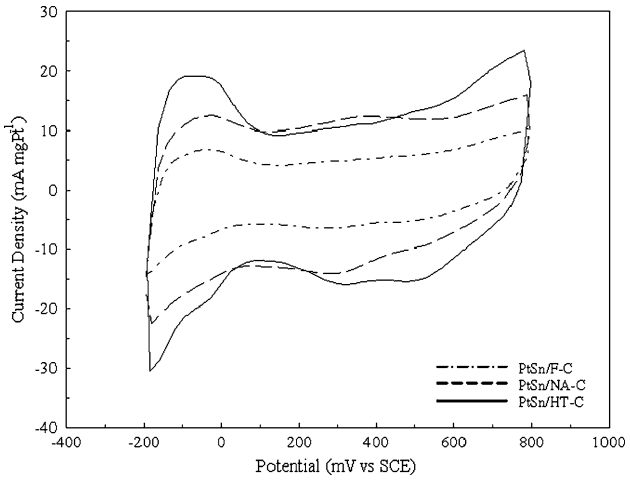

Fig. 4 Cyclic voltammograms of the synthesized PtSn/C catalysts in 0.5 M H_2SO_4 solution with a scan rate of 50 mV s^{-1} at 25 °C

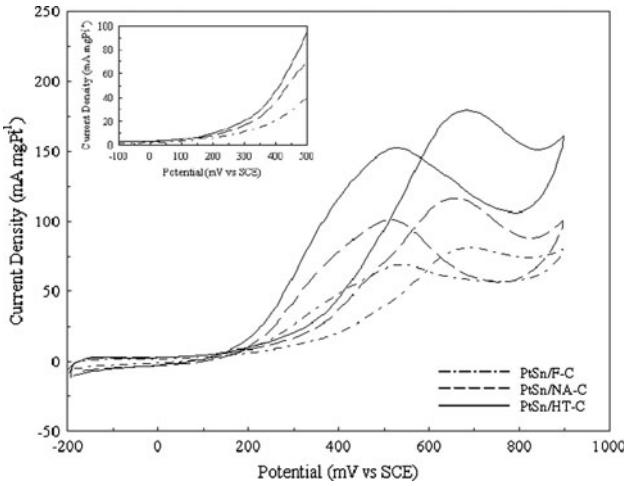

Fig. 5 Cyclic voltammograms of the synthesized PtSn/C catalysts in 0.5 M H_2SO_4 containing 1 M CH_3CH_2OH solution with a scan rate of 20 mV s^{-1} at 25 °C

the highest amount of available Pt active sites, inferring the better Pt dispersion in the PtSn/HT-C. Similarly, the much lower ESA of PtSn/F-C and PtSn/NA-C could be attributed to an inadequate Pt active sites dispersed on the untreated/acid-treated supports as well as the bigger Pt particle sizes in those catalysts obtained from TEM. As a result, the PtSn/HT-C showed higher catalytic activity than the others did.

Figure 5 presents the cyclic voltammograms of the as-prepared PtSn/C catalysts toward ethanol oxidation. As can be seen, there are two oxidation peaks in the potential window of −200 to 900 mV/SCE. The first oxidation peak appears during the forward scan, and the one on the left in the reverse scan. No hydrogen ad/desorption peaks can be observed, due to prominence of ethanol adsorption. The inset in Fig. 5 shows the onset potential of PtSn/F-C, PtSn/NA-C and PtSn/HT-C, which are 220, 175 and 160 mV/SCE, respectively. As reported in the other work [34], the onset potential of the commercial Pt/C was 510 mV/SCE. Thus, the addition of Sn to Pt led to the negative onset potential, approximately 300 mV/SCE, indicating easier and faster ethanol oxidation in those binary catalysts. The peak potential of the as-prepared PtSn/C catalysts was in the range of 650–690 mV/SCE during the positive potential scanning and 510–540 mV/SCE for their reverse scanning, respectively. The activity of the catalysts for ethanol oxidation is normally determined by the maximum current density of the positive scan peak [8]. From the voltammograms, the maximum current density of all those binary catalysts was ranked as follows: PtSn/HT-C (179.5 mA $mgPt^{-1}$) > PtSn/NA-C (116.6 mA $mgPt^{-1}$) > PtSn/F-C (81.3 mA $mgPt^{-1}$). As a result, the PtSn/HT-C catalyst provided the highest electrochemical activity for ethanol oxidation, possibly resulting from its highest ESA.

It was also observed that the maximum current density obtained from PtSn/HT-C was about 1.5 times that from PtSn/NA-C although the ESA of PtSn/HT-C was five times that of the PtSn/NA-S. This is because the Pt:Sn ratio and the oxide form of Sn play important roles for ethanol oxidation. This result is similar to the finding in the previous work carried out by Spinace et al. [35]. The presence of Sn can promote ethanol oxidation not only by an electronic effect in the Pt-based electrode material but also by an activation of the interfacial water molecules necessary to promote CO and acetaldehyde oxidation reactions [4, 7]. The Pt:Sn ratio in PtSn/NA-C was about 4.74:1 which is closer to 3:1 than that of PtSn/HT-C. The optimum ratio of Pt:Sn giving the best DEFC performance previously reported was 3 or approaching 3 [7, 12]. In addition, Zhou et al. [8] presented that the DEFC anode catalyst containing lower Pt:Sn ratio showed better cell performance than that with higher Pt:Sn ratio.

To confirm the catalytic activity of the as-prepared PtSn/C catalysts toward ethanol oxidation, chronoamperometric experiment was conducted by holding the potential at 600 mV/SCE for 30 min in 0.5 M H_2SO_4 containing 1 M CH_3CH_2OH; and the result shows in Fig. 6. As seen from Fig. 6, the current of all binary catalysts drops rapidly within 5 min, and then decays slowly. After holding the potential for 30 min, the final current density of PtSn/F-C, PtSn/NA-C and PtSn/HT-C catalysts were 23.1, 28.2 and 47.5 mA $mgPt^{-1}$, respectively. This result indicated that PtSn/HT-C catalyst had stronger tolerance to the poisoning adsorbed CO species, implying better catalytic activity for ethanol oxidation as compared to the other PtSn/C catalysts. The results are in agreement with those of cyclic voltammetry measurements.

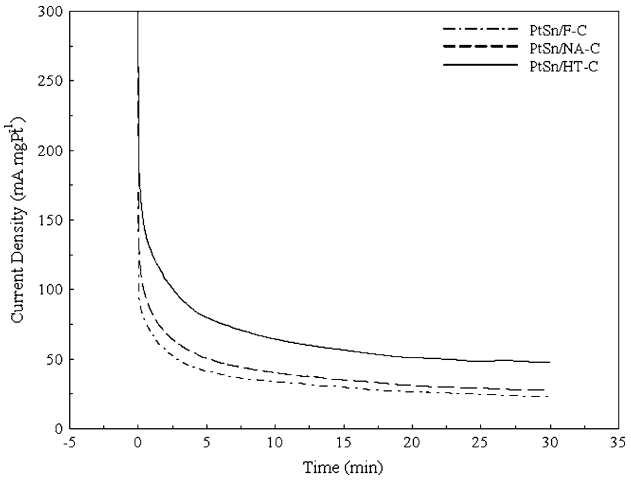

Fig. 6 Chronoamperometric curves of the as-prepared PtSn/C catalysts in 0.5 M H_2SO_4 containing 1 M CH_3CH_2OH solution at 600 mV/SCE for 30 min

3.4 Electrochemistry test for EOR of PtSn/C catalysts at the same Pt loading

To verify the effects of the pre-treatment method of the support towards an EOR, the electrochemical characterization of the as-prepared PtSn on the different pretreated supports were performed again by keeping the same amount of Pt loaded on to a glassy support. The voltammograms in 0.5 M H_2SO_4 with/without 1 M CH_3CH_2OH and the chronoamperometric curves in 0.5 M H_2SO_4 containing 1 M CH_3CH_2OH are illustrated in Fig. 7. As seen from Fig. 7a, PtSn/HT-C catalyst provided a larger hydrogen desorption area. As a consequence, it would have a higher ESA. The ESA of PtSn/HT-C was 57.4 $m^2\ g^{-1}$ which is much higher than those of PtSn/NA-C and PtSn/F-C. PtSn/HT-C also showed superior ethanol oxidation and CO tolerance to the other as-prepared PtSn/C catalysts, as displayed the results in Fig. 7b, c respectively. By comparing between the results at the constant catalyst loading and the constant Pt loading, PtSn/HT-C still gave higher performance than PtSn/NA-C, while PtSn/F-C had the lowest performance in ethanol oxidation. This is a compromise effect of Pt dispersion and Pt:Sn ratio. PtSn/NA-C contained higher Sn:Pt ratio while PtSn/HT-C had higher Pt dispersion.

3.5 Direct ethanol fuel cell test

The DEFC performances of the cell, prepared from the as-prepared PtSn/C catalysts employed as anode catalysts, are displayed in Fig. 8. Since the Pt amounts deposited on the pre-treated and untreated supports were not the same

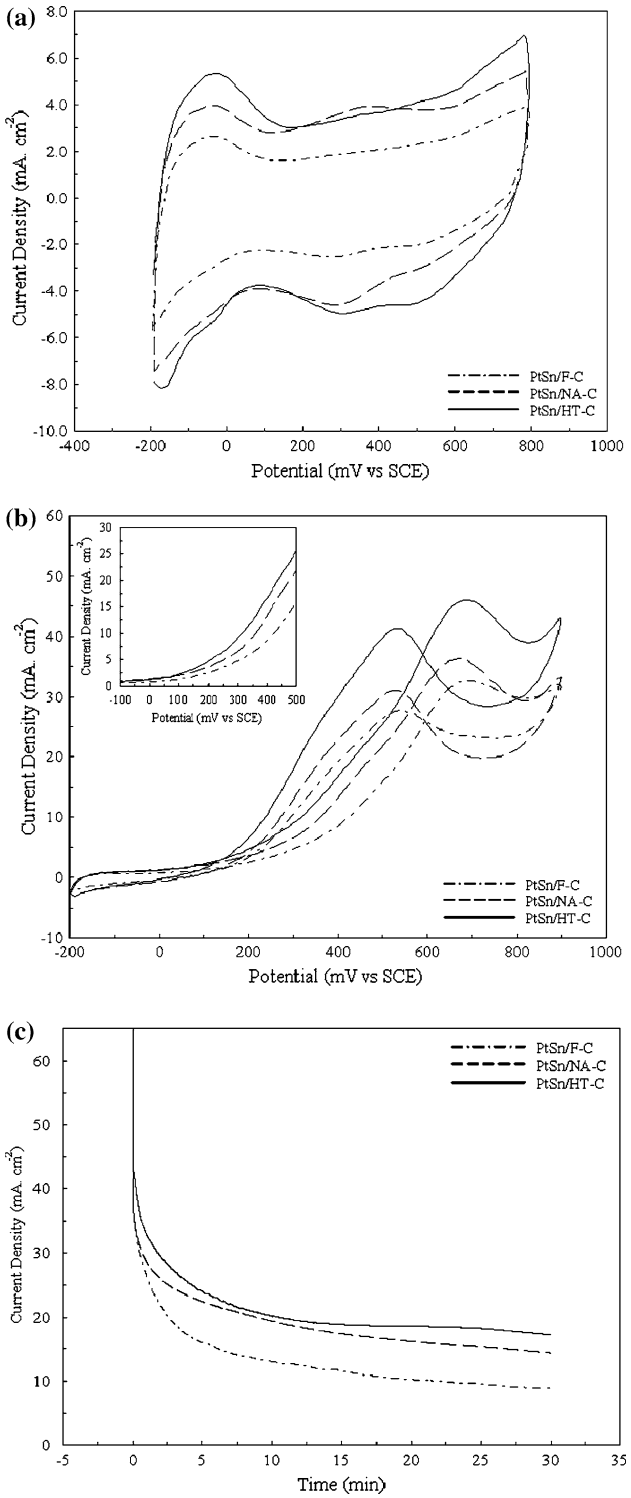

Fig. 7 Electrochemistry curves of the PtSn/C electrocatalysts loaded at the same amount of Pt on a glassy carbon at 25 °C: **a** Voltammograms in 0.5 M H_2SO_4 with a scan rate of 50 mV s^{-1}, **b** Voltammograms in 0.5 M H_2SO_4 + 1 M C_2H_5OH with a scan rate of 20 mV s^{-1}, **c** Chronoamperometric curves in 0.5 M H_2SO_4 + 1 M C_2H_5OH at 600 mV/SCE for 30 min

as previously mentioned, the polarization and power density curves of these electrodes were calculated, based on the weight of Pt in units of mA $mgPt^{-1}$ instead of mA cm^{-2} to account for the effect of different amounts of Pt (Fig. 8). To verify the role of Sn in the binary catalysts, polarization and power density curves of the commercial Pt/C were used for comparison. The I–V curves show that the open circuit voltages of all the binary catalysts were about 720 mV, which is noticeably higher than that of Pt/C, which was at approximately 300 mV. The I–V curves of Pt/C showed that the voltage sharply dropped as the current density increased, demonstrating much faster poisoning of the Pt active sites in Pt/C than in the as-prepared PtSn/C catalysts. In contrast, the enhanced performance of all the binary catalysts was attributed to the incorporation of Sn into Pt, promoting oxidative removal of the poisoning CO species by the so-called bi-functional mechanism.

The maximum power density of all the catalysts is ranked from the highest to the lowest as follows: PtSn/HT-C > PtSn/NA-C > PtSn/F-C > Pt/C, which is in reasonable agreement with the activity of these catalysts towards the EOR that was obtained from cyclic voltammetry and chronoamperometry techniques. In the low current density region (<75 mA cm^{-2}), slightly better performance of PtSn/NA-C than PtSn/HT-C and PtSn/F-C was observed, which might have been due to the contribution of the higher Sn:Pt ratio obtained from PtSn/NA-C catalyst preparation. It was also observed that the performance of PtSn/NA-C was diminished by the higher current density region but was still better than that of PtSn/F-C. It was believed that the HNO_3 pretreatment of support could generate significant surface oxygen complexes, which had enhanced the hydrophilicity of the carbon [23]. This could have prevented the gas (CO_2) product from being released from the catalyst layer, resulting in inhibition of fuel accessibility to the active sites [36]. As a result, PtSn/HT-C enhanced both DEFC performance as well as catalytic activity towards ethanol oxidation. This could be explained by the thermal pre-treatment approach of support having improved metal dispersion, as was shown in the TEM images, and could have led to a high electrochemical surface area for ethanol oxidation. Overall, our results indicated that considerable increase in the ethanol oxidation reaction (EOR) over the PtSn/C catalyst can be achieved by pretreatment of the support, and of the prepared electrocatalysts, the PtSn/HT-C showed the best DEFC performance.

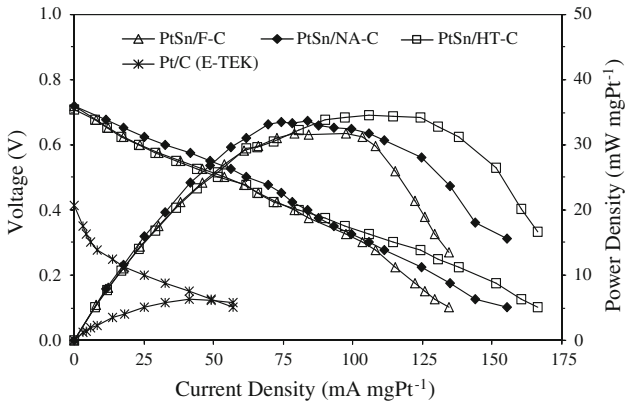

Fig. 8 Normalized DEFC performance curves by actual amount of Pt noble metal

4 Conclusion

This study, the effect of pre-treatment methods of carbon supports for PtSn on catalytic activity of the prepared PtSn/C catalysts was investigated. Both acid and thermal activation methods affected the surface characteristics of the supports differently, including specific surface area, pore size, surface functional groups, and surface charge. The surface characteristics of the supports determined metal loading and interaction between the metal precursor and the support surface during the deposition step. FTIR spectra showed that the HNO_3 pre-treatment had produced various oxygenated functional groups such as phenol, quinone, carboxyl-carbonates, and nitrate groups on the support surface, which promotes acidic property. The high acidic functional groups on NA-C could hinder Pt reduction but promote Sn deposition leading to lower Pt:Sn ratio. By contrast, thermal activation enhanced the specific surface area of the carbon and increased base functional groups. The base functional groups acted as the sites for Pt nanocluster deposition and consequently provided smaller metal particle sizes and higher metal dispersion resulting in higher Pt:Sn ratio. The cyclic voltammograms in sulfuric acid and chronoamperometric results revealed that the PtSn/HT-C catalyst had yielded the highest electrochemical surface area and electrochemical activity for ethanol oxidation, respectively. As a result, heat treatment of carbon had enhanced catalytic activity for ethanol oxidation, as well as DEFC performance, of the PtSn/C catalyst better than nitric acid treatment would have done, owing to a combination of high metal dispersion and suitable Pt:Sn ratio.

Acknowledgments The authors are grateful for the financial support of the Thailand Research Fund (TRF) for the academic Royal Golden Jubilee (RGJ) scholarship. The authors also wish to thank the Joint Graduate School of Environmental and Energy of King Mongkut's University Technology Thonburi for providing the electrochemical measurement apparatus.

References

1. Lamy C, Lima A, LeRhun V, Delime F, Coutanceau C, Léger J-M (2002) J Pow Sour 105:283
2. Song SQ, Tsiakaras P (2006) Appl Catal B 63:187
3. Song SQ, Zhou WJ, Liang ZX, Cai R, Sun GQ, Xin Q, Stergiopoulos V, Tsiakaras P (2005) Appl Catal B 55:65
4. Simões FC, dos Anjos DM, Vigier F, Léger J-M, Hahn F, Coutanceau C, Gonzalez ER, Tremiliosi-Filho G, de Andrade AR, Olivi P, Kokoh KB (2007) J Pow Sour 167:1
5. Rousseau S, Coutanceau C, Lamy C, Léger J-M (2006) J Pow Sour 158:18
6. Antolini E (2007) J Pow Sour 170:1
7. Jiang LH, Colmenares L, Jusys Z, Sun GQ, Behm RJ (2007) Electrochim Acta 53:377
8. Zhou WJ, Zhou ZH, Song SQ, Li WZ, Sun GQ, Tsiakaras P, Xin Q (2003) Appl Catal B 46:273
9. Liu ZL, Ling XY, Su XD, Lee JY, Gan LM (2005) J Pow Sour 149:1
10. Wang ZB, Yin GP, Zhang J, Sun YC, Shi PF (2006) J Pow Sour 160:37
11. Jiang LH, Sun GQ, Zhou ZH, Zhou WJ, Xin Q (2004) Catal Today 93–95:665
12. Guo YL, Zheng YZ, Huang MH (2008) Electrochim Acta 53:3102
13. Neto AO, Farias LA, Dias RR, Brandalise M, Linardi M, Spinace EV (2008) Electrochem Commun 10:1315
14. Tsiakaras PE (2007) J Pow Sour 171:107
15. dos Anjos DM, Kokoh KB, Léger J-M, de Andrade AR, Olivi P, Tremiliosi-Filho G (2006) J Appl Electrochem 36:1391
16. Colmati F, Antolini E, Gonzalez ER (2008) J Alloys Compd 456:264
17. Lima FHB, Gonzalez ER (2008) Electrochim Acta 53:2963
18. Lamy C, Rousseau S, Belgsir EM, Coutanceau C, Léger J-M (2004) Electrochim Acta 49:3901
19. Colmati F, Antolini E, Gonzalez ER (2006) J Pow Sour 157:98
20. Neto AO, Dias RR, Tusi MM, Linardi M, Spinace EV (2007) J Pow Sour 166:87
21. Jiang LH, Sun GQ, Sun SG, Liu JG, Tang SH, Li HQ, Zhou B, Xin Q (2005) Electrochim Acta 50:5384
22. Antolini E (2009) Appl Catal B 88:1
23. Tian JH, Wang FB, Shan ZHQ, Wang RJ, Zhang JY (2004) J Appl Electrochem 34:461
24. Reymond JP, Kolenda F (1999) Powder Technol 103:30
25. Kim S, Park SJ (2007) Electrochim Acta 52:3013
26. Jiang LH, Sun GQ, Zhou ZH, Sun SG, Wang Q, Yan SY, Li HQ, Tian J, Guo JS, Zhou B, Xin Q (2005) J Phys Chem B 109:8774
27. Thepkaew J, Therdthianwong A, Therdthianwong S (2008) Energy 33:1794
28. Wang SB, Max Lu GQ (1998) Carbon 36:283
29. Chen JP, Wu SN (2004) Langmuir 20:2233
30. Coloma F, Escribano AS, Reinoso FR (1995) J Catal 154:299
31. Scibioh MA, Oh IH, Lim TH, Hong SA, Ha HY (2008) Appl Catal B 77:373
32. Figueiredo JL, Pereira MFR, Freitas MMA, Orfao JJM (1999) Carbon 37:1379
33. Li HQ, Sun GQ, Cao L, Jiang LH, Xin Q (2007) Electrochim Acta 52:6622
34. Song HQ, Qiu XP, Li FH, Zhu WT, Chen LQ (2007) Electrochem Commun 9:1416
35. Spinace EV, Linardi M, Neto AO (2005) Electrochem Commun 7:365
36. Surampudi S (1993) US Patent 5,599,638